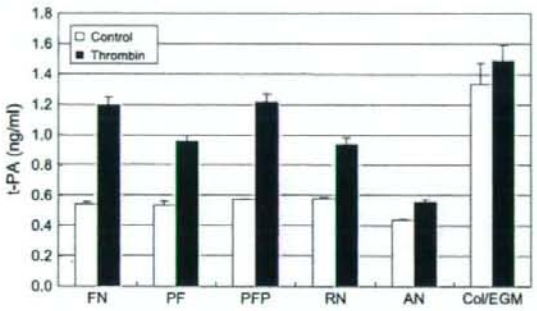

Fig. 7. Effects of cell adhesive proteins on the thrombin- stimulated production of tissue plasminogen activator. HUVECs were seeded at 7×10^4 cells/well on 24-well plates previously coated with Fibronectin (FN), Pronectin F (PF), Pronectin F PLUS (PFP), Retronectin (RN), or Attachin (AN). After culturing for 1 day, the cells were stimulated with 1 U/ml of thrombin. After 24 h incubation, the conditioned media were collected and t-PA concentration was determined by enzyme immunoassay. Results are expressed as nanograms of t-PA/ml of the supernatant and represent the mean ± S.D. of triplicate determinations. t-PA production from HUVECs cultured in serum-containing growing media (EGM-2) plated on collagen-coated dish was also examined (Col/EGM).

[47–50]. The culture conditions for OECs and for tissue-derived endothelial cells such as HUVECs are the same: endothelial basal media supplemented with fetal calf serum, VEGF, basic FGF, IGF-1, EGF and ascorbic acid. Fibronectin is the cell adhesion protein most commonly used to obtain OECs. Therefore, examining the usefulness of recombinant cell adhesion proteins as a substitute for plasma fibronectin in serum-free culture would lead to the establishment of a serum-free culture for OECs as well.

The cell culture method chosen has a direct influence on the quality and safety of cellular therapy products. The composition of media and serum are considered to affect the features of the cells, and animal-derived materials are known to carry the risk of infection or allergy. Thus, developing appropriate culture methods and ways of evaluating these methods are key to assuring the safety of cellular therapy products [11,12]. For example, when culturing human embryonic stem cells that are anticipated to be a useful source for cellular therapy products, non-human-type sialic acid (*N*-glycolyl neuraminic acid) derived from animal serum is incorporated into the sugar chain on the cell surface, which could induce an immune response

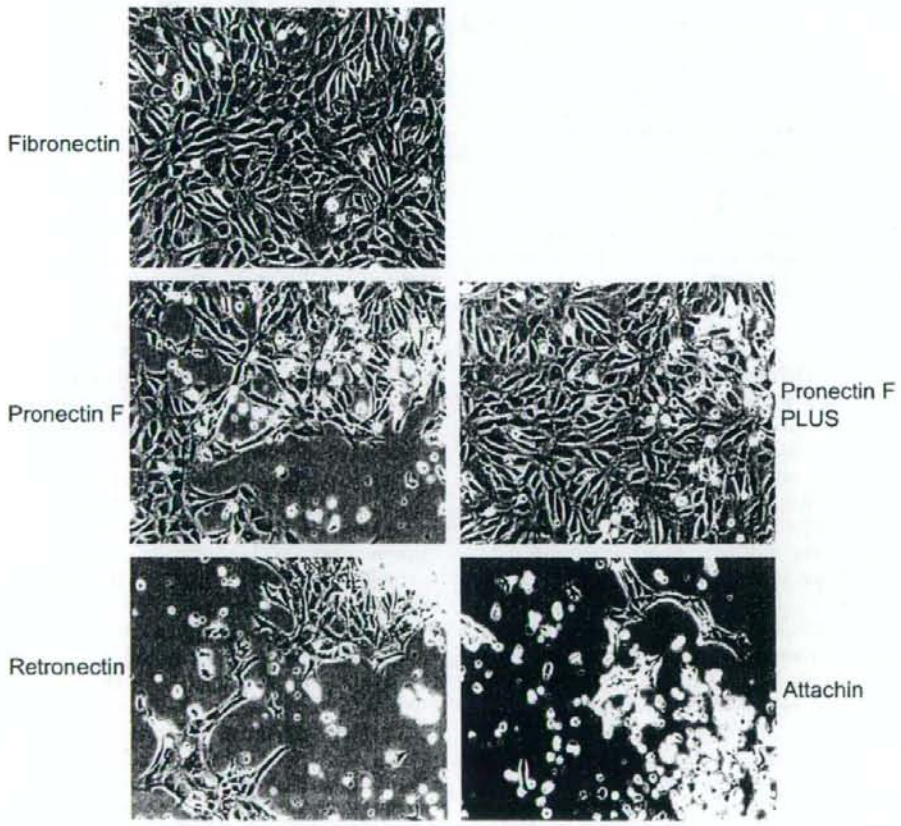

Fig. 8. Detachment of HUVECs cultured in the presence of thrombin. Cells were plated on the plates previously coated with Fibronectin, Pronectin F, Pronectin F PLUS, Retronectin, or Attachin, and cultured for 24 h in the presence of 1 U/ml of thrombin. The cells were photographed before harvesting the supernatant that is provided for the measurement of the t-PA concentration.

upon transplantation [51]. In addition, the transmission of unknown viruses from rodent feeder cells is also a concern [8]. Therefore, establishing cell culture methods that assure safety is an important goal in the development of cellular therapy products.

Because recombinant proteins can be produced without using animal or human-derived materials, providing the protein factors that are necessary to cell culture as recombinant proteins can contribute to improving the safety of cellular therapy products. Recombinant proteins also have an advantage in that they can provide consistent performance from lot to lot, and their function can be modified by molecular design. Artificial recombinant proteins have the possibility of being superior to naturally occurring proteins; for example, Retronectin, a deletion mutant of fibronectin that unfortunately showed less activity as an adhesive protein in this study, is much more effective in supporting gene transfer by retrovirus vectors than fibronectin [23]. If there is a concern in using artificial recombinant proteins, the residual artificial protein has the potential to show immunogenicity.

In our experiments to test cell adhesion, Pronectin F and Pronectin F PLUS were superior to fibronectin when they were used in lower concentrations (Fig. 1). This might be because both Pronectin F and Pronectin F PLUS have 13 repeats of the RGD sequence in one molecule, whereas fibronectin has only two. Pronectin F and Pronectin F PLUS are also structurally stable, and thus the coated substrates retain their performance for at least 2 years at room temperature, which is another advantage over fibronectin [52]. Pronectins were produced without using any animal-derived components (Dr. Kurokawa, Sanyo Kasei Kogyo, personal communication).

Pronectin F is not soluble in water since the silk-like protein sequence forms strong hydrogen bonds intermolecularly; thus, it must be dissolved in $LiClO_4$ [21]. Therefore, Pronectin F PLUS, a water-soluble variant of Pronectin F, was developed by chemical modification of the serine residues of Pronectin F [22]. As shown in Fig. 3, a higher amount of Pronectin F was absorbed on polystyrene dishes than Pronectin F PLUS. Since the surface of polystyrene plates is hydrophobic, hydrophobic Pronectin F might have been absorbed well. Pronectin L, which has a similar core sequence to that of Pronectin F, was also absorbed well on the dish, although no cells adhered on it.

In spite of their differences in absorption on the polystyrene dish, Pronectin F PLUS and Pronectin F showed similar efficiency with respect to the adhered cell number, growth support, induction of FAK phosphorylation, and production of PGI_2 and t-PA. Moreover, Pronectin F PLUS was more potent than Pronectin F in its support of cell adhesion under stimulation with thrombin (Fig. 9). The cells on Pronectin F PLUS were resistant to cell detachment due to the thrombin-induced cytoskeletal changes. This might be because that Pronectin F PLUS is positively charged by chemical modification. Since the cell surface possesses a negative charge, the adhesive intensity between the cells and Pronectin F PLUS was increased due to the static electrical interaction, resulting in the maintenance of cell adhesiveness after the cytoskeletal change

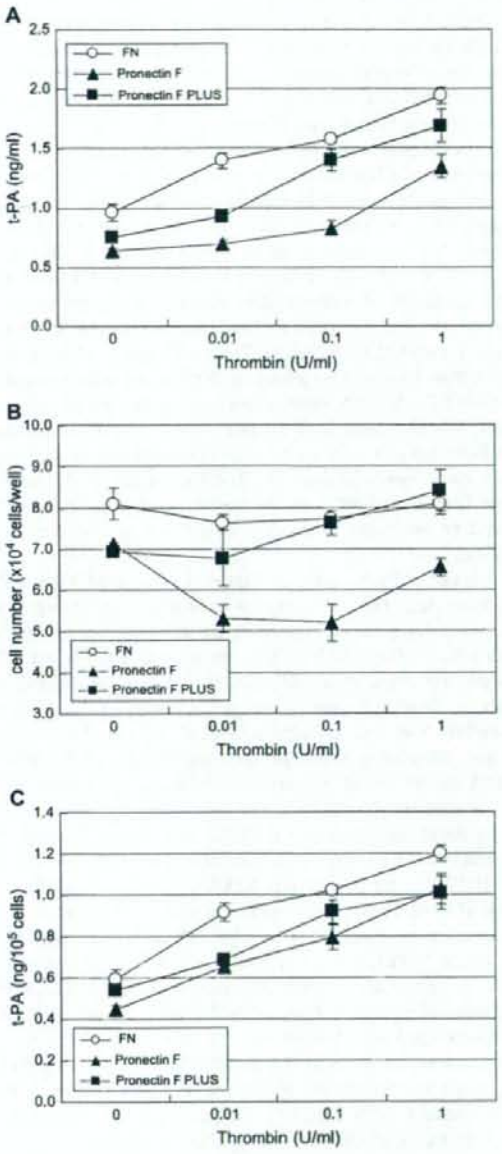

Fig. 9. Thrombin-induced production of t-PA and decrease in viability of HUVECs adhered on Pronectin F. HUVECs were seeded at 7×10^4 cells/well on 24-well plates previously coated with Fibronectin, Pronectin F or Pronectin F PLUS. After culturing for 1 day, the cells were stimulated with thrombin at the indicated concentrations. After 24 h incubation, the conditioned media were collected and t-PA concentration was determined by enzyme immunoassay (A). The cell numbers were determined using a Cell-Counting Kit-8 (B). Production of t-PA per 10^5 cells was calculated (C). Each data point represents the mean ± S.D. of triplicate determinations.

induced by thrombin. To our knowledge, this is the first observation to reveal the difference in biological properties between Pronectin F and Pronectin F PLUS. The retention of human endothelial cells on the lumen in the presence of physiological stimuli is an important prerequisite for artificial artery grafts to be successful, and, therefore, Pronectin F PLUS could also be suited for use in this type of graft.

In the present study, the usefulness of Pronectin F PLUS as a substitute for fibronectin was indicated; however, Pronectin F PLUS and Pronectin F were less effective than fibronectin in long-term cell cultures. We were able to culture HUVECs up to around 6 passages using the serum-free media with fibronectin. However, when Pronectin F or Pronectin F PLUS was used instead of fibronectin, the cell number did not increase beyond the second passage. Although Pronectin F PLUS worked better than Pronectin F, the efficiency of both was lower than that of fibronectin in the long-term maintenance of HUVECs. Since fibronectin has several functional domains that can bind to heparin, fibrin and collagen, signals other than the RGD-integrin interaction would be important in the long-term maintenance of the cells. The incorporation of domains other than that of RGD of fibronectin into Pronectin F PLUS would be necessary to improve its efficacy in long-term cell cultures.

For cell cultures, porcine trypsin is often used when cells are harvested. The use of trypsin may lead to the contamination of animal-derived materials or transmissible agents. In serum-free cultures of HUVECs, we were able to harvest cells for passage using a protease free of animal-derived materials such as TrypLE Select (Invitrogen, Carlsbad, CA, USA) or AccuMax (Chemicon, Billerica, MA, USA); therefore, trypsin is not necessarily used for the maintenance of HUVECs, which means that it is possible to eliminate the potential for contamination of animal-derived proteins.

In summary, Pronectin F PLUS was shown to have the closest activity to plasma fibronectin in the serum-free culture of HUVECs by examining VEGF- or bFGF-induced cell proliferation, FAK phosphorylation, and thrombin-stimulated production of PGI_2 or t-PA. The cell adherent activity of Pronectin F PLUS was superior to fibronectin at concentrations of less than 1 μg/ml. Although Pronectin F PLUS has the same amino acid sequence as Pronectin F, only HUVECs on Pronectin F PLUS were resistant to thrombin-induced cell detachment. Pronectin F PLUS is thus thought to be a promising substitute for plasma fibronectin in the serum-free culture of endothelial cells, although modification would be necessary to improve its efficiency in long-term cell cultures.

Acknowledgements

This work was supported in part by a Grant-in-Aid for Health and Labor Science Research (H17-SAISEI-021 and H17-IYAKU-015) from the Japanese Ministry of Health, Labor and Welfare, and a Grant-in-Aid for Young Scientists (B) from the Ministry of Education, Science, Sports and Culture.

References

[1] Wollert KC, Drexler H. Cell-based therapy for heart failure. Curr Opin Cardiol 2006;21:234–9.
[2] Zavos PM. Stem cells and cellular therapy: potential treatment for cardiovascular diseases. Int J Cardiol 2006;107:1–6.
[3] Fazel S, Tang GH, Angoulvant D, Cimini M, Weisel RD, Li RK, et al. Current status of cellular therapy for ischemic heart disease. Ann Thorac Surg 2005;79:S2238–47.
[4] http://www.fda.gov/cber/gdlns/somgene.pdf.
[5] http://www.fda.gov/cber/gdlns/cmcsomcell.pdf.
[6] http://www.emea.eu.int/pdfs/human/cpwp/32377405en.pdf.
[7] http://www.fda.gov/cber/rules/suitdonor.pdf.
[8] Lee JB, Lee JE, Park JH, Kim SJ, Kim MK, Roh SI, et al. Establishment and maintenance of human embryonic stem cell lines on human feeder cells derived from uterine endometrium under serum-free condition. Biol Reprod 2005;72:42–9.
[9] Ogawa K, Matsui H, Ohtsuka S, Niwa H. A novel mechanism for regulating clonal propagation of mouse ES cells. Genes Cells 2004;9:471–7.
[10] Asher DM. Bovine sera used in the manufacture of biologicals: current concerns and policies of the U.S. Food and Drug Administration regarding the transmissible spongiform encephalopathies. Dev Biol Stand 1999; 99:41–4.
[11] Asher DM. The transmissible spongiform encephalopathy agents: concerns and responses of United States regulatory agencies in maintaining the safety of biologics. Dev Biol Stand 1999;100:103–18.
[12] Cobo F, Stacey GN, Hunt C, Cabrera C, Nieto A, Montes R, et al. Microbiological control in stem cell banks: approaches to standardisation. Appl Microbiol Biotechnol 2005;68:456–66.
[13] Cobo F, Talavera P, Concha A. Diagnostic approaches for viruses and prions in stem cell banks. Virology 2006;347:1–10.
[14] Kornblihtt AR, Umezawa K, Vibe-Pedersen K, Baralle FE. Primary structure of human fibronectin: differential splicing may generate at least 10 polypeptides from a single gene. EMBO J 1985;4:1755–9.
[15] Umezawa K, Kornblihtt AR, Baralle FE. Isolation and characterization of cDNA clones for human liver fibronectin. FEBS Lett 1985;186:31–4.
[16] Pierschbacher MD, Ruoslahti E. Cell attachment activity of fibronectin can be duplicated by small synthetic fragments of the molecule. Nature 1984;309:30–3.
[17] Ruoslahti E, Pierschbacher MD. New perspectives in cell adhesion: RGD and integrins. Science 1987;238:491–7.
[18] Bourdoulous S, Orend G, MacKenna DA, Pasqualini R, Ruoslahti E. Fibronectin matrix regulates activation of RHO and CDC42 GTPases and cell cycle progression. J Cell Biol 1998;143:267–76.
[19] Frisch SM, Ruoslahti E. Integrins and anoikis. Curr Opin Cell Biol 1997;9:701–6.
[20] Heslot H. Artificial fibrous proteins: a review. Biochimie 1998;80:19–31.
[21] Cappello J. Genetically Engineered Protein Polymers. In: Domb AJ, Kost J, Wiseman D, editors. Handbook of Biodegradable Polymers. Amsterdam: Harwood Academic Publishers; 1997. p. 387–416.
[22] Hosseinkhani H, Tabata Y. PEGylation enhances tumor targeting of plasmid DNA by an artificial cationized protein with repeated RGD sequences, Pronectin. J Control Release 2004;97:157–71.
[23] Hanenberg H, Xiao XL, Dilloo D, Hashino K, Kato I, Williams DA. Colocalization of retrovirus and target cells on specific fibronectin fragments increases genetic transduction of mammalian cells. Nat Med 1996;2:876–82.
[24] http://home.kimo.com.tw/biotaichchen/Attachin/into.html.
[25] http://home.kimo.com.tw/biotaichchen/Attachin/qa.html.
[26] Gorfien S, Spector A, DeLuca D, Weiss S. Growth and physiological functions of vascular endothelial cells in a new serum-free medium (SFM). Exp Cell Res 1993;206:291–301.
[27] Zaric J, Ruegg C. Integrin-mediated adhesion and soluble ligand binding stabilize COX-2 protein levels in endothelial cells by inducing expression and preventing degradation. J Biol Chem 2005;280:1077–85.
[28] Ilic D, Kovacic B, Johkura K, Schlaepfer DD, Tomasevic N, Han Q, et al. FAK promotes organization of fibronectin matrix and fibrillar adhesions. J Cell Sci 2004;117:177–87.

[29] Almeida EA, Ilic D, Han Q, Hauck CR, Jin F, Kawakatsu H, et al. Matrix survival signaling: from fibronectin via focal adhesion kinase to c-Jun NH(2)-terminal kinase. J Cell Biol 2000;149:741–54.
[30] Schlaepfer DD, Broome MA, Hunter T. Fibronectin-stimulated signaling from a focal adhesion kinase-c-Src complex: involvement of the Grb2, p130cas, and Nck adaptor proteins. Mol Cell Biol 1997;17:1702–13.
[31] Ruest PJ, Roy S, Shi E, Mernaugh RL, Hanks SK. Phosphospecific antibodies reveal focal adhesion kinase activation loop phosphorylation in nascent and mature focal adhesions and requirement for the autophosphorylation site. Cell Growth Differ 2000;11:41–8.
[32] Fuchs S, Motta A, Migliaresi C, Kirkpatrick CJ. Outgrowth endothelial cells isolated and expanded from human peripheral blood progenitor cells as a potential source of autologous cells for endothelialization of silk fibroin biomaterials. Biomaterials 2006;27:5399–408.
[33] Jain RK, Au P, Tam J, Duda DG, Fukumura D. Engineering vascularized tissue. Nat Biotechnol 2005;23:821–3.
[34] Levenberg S, Rouwkema J, Macdonald M, Garfein ES, Kohane DS, Darland DC, et al. Engineering vascularized skeletal muscle tissue. Nat Biotechnol 2005;23:879–84.
[35] Koike N, Fukumura D, Gralla O, Au P, Schechner JS, Jain RK. Tissue engineering: creation of long-lasting blood vessels. Nature 2004;428:138–9.
[36] Meinhart JG, Schense JC, Schima H, Gorlitzer M, Hubbell JA, Deutsch M, et al. Enhanced endothelial cell retention on shear-stressed synthetic vascular grafts precoated with RGD-cross-linked fibrin. Tissue Eng 2005;11:887–95.
[37] Julkunen I, Hautanen A, Keski-Oja J. Interaction of viral envelope glycoproteins with fibronectin. Infect Immun 1983;40:876–81.
[38] Torre D, Pugliese A, Ferrario G, Marietti G, Forno B, Zeroli C. Interaction of human plasma fibronectin with viral proteins of human immunodeficiency virus. FEMS Immunol Med Microbiol 1994;8:127–31.
[39] Merx MW, Zernecke A, Liehn EA, Schuh A, Skobel E, Butzbach B, et al. Transplantation of human umbilical vein endothelial cells improves left ventricular function in a rat model of myocardial infarction. Basic Res Cardiol 2005;100:208–16.
[40] Fuchs S, Hermanns MI, Kirkpatrick CJ. Retention of a differentiated endothelial phenotype by outgrowth endothelial cells isolated from human peripheral blood and expanded in long-term cultures. Cell Tissue Res 2006;326:79–92.
[41] Cai H, Gehrig P, Scott TM, Zimmermann R, Schlapbach R, Zisch AH. MnSOD marks cord blood late outgrowth endothelial cells and accompanies robust resistance to oxidative stress. Biochem Biophys Res Commun 2006;350:364–9.
[42] Sharpe 3rd EE, Teleron AA, Li B, Price J, Sands MS, Alford K, et al. The origin and in vivo significance of murine and human culture-expanded endothelial progenitor cells. Am J Pathol 2006;168:1710–21.
[43] Gulati R, Jevremovic D, Peterson TE, Chatterjee S, Shah V, Vile RG, et al. Diverse origin and function of cells with endothelial phenotype obtained from adult human blood. Circ Res 2003;93:1023–5.
[44] Lin Y, Weisdorf DJ, Solovey A, Hebbel RP. Origins of circulating endothelial cells and endothelial outgrowth from blood. J Clin Invest 2000; 105:71–7.
[45] Smadja DM, Bieche I, Uzan G, Bompais H, Muller L, Boisson-Vidal C, et al. PAR-1 activation on human late endothelial progenitor cells enhances angiogenesis in vitro with upregulation of the SDF-1/CXCR4 system. Arterioscler Thromb Vasc Biol 2005;25:2321–7.
[46] Eggermann J, Kliche S, Jarmy G, Hoffmann K, Mayr-Beyrle U, Debatin KM, et al. Endothelial progenitor cell culture and differentiation in vitro: a methodological comparison using human umbilical cord blood. Cardiovasc Res 2003;58:478–86.
[47] Hur J, Yoon CH, Kim HS, Choi JH, Kang HJ, Hwang KK, et al. Characterization of two types of endothelial progenitor cells and their different contributions to neovasculogenesis. Arterioscler Thromb Vasc Biol 2004;24:288–93.
[48] Yoon CH, Hur J, Park KW, Kim JH, Lee CS, Oh IY, et al. Synergistic neovascularization by mixed transplantation of early endothelial progenitor cells and late outgrowth endothelial cells: the role of angiogenic cytokines and matrix metalloproteinases. Circulation 2005;112: 1618–27.
[49] Ott I, Keller U, Knoedler M, Gotze KS, Doss K, Fischer P, et al. Endothelial-like cells expanded from CD34+ blood cells improve left ventricular function after experimental myocardial infarction. FASEB J 2005; 19:992–4.
[50] Choi JH, Hur J, Yoon CH, Kim JH, Lee CS, Youn SW, et al. Augmentation of therapeutic angiogenesis using genetically modified human endothelial progenitor cells with altered glycogen synthase kinase-3beta activity. J Biol Chem 2004;279:49430–8.
[51] Martin MJ, Muotri A, Gage F, Varki A. Human embryonic stem cells express an immunogenic nonhuman sialic acid. Nat Med 2005;11: 228–32.
[52] http://www.sanyo-chemical.co.jp/product/pronectin/eng/prodspec.htm.

J Pharmacol Sci 103, 159 – 167 (2007)

Journal of Pharmacological Sciences

Full Paper

Caspase Cascade Proceeds Rapidly After Cytochrome *c* Release From Mitochondria in Tumor Necrosis Factor-α-Induced Cell Death

Hiroshi Kawai[1,3,*], Takuo Suzuki[1], Tetsu Kobayashi[1], Akiko Ishii-Watabe[1], Haruna Sakurai[2], Hisayuki Ohata[2], Kazuo Honda[2], Kazutaka Momose[2], Takao Hayakawa[1], and Toru Kawanishi[1,#]

[1]*Division of Biological Chemistry and Biologicals, National Institute of Health Sciences, Tokyo 158-8501, Japan*
[2]*Department of Pharmacology, School of Pharmaceutical Sciences, Showa University, Tokyo 142-8555, Japan*
[3]*Faculty of Pharmaceutical Sciences, Josai International University, Chiba 283-8555, Japan*

Received August 2, 2006; Accepted December 2, 2006

Abstract. The caspase activation cascade and mitochondrial changes are major biochemical reactions in the apoptotic cell death machinery. We attempted to clarify the temporal relationship between caspase activation, cytochrome *c* release, mitochondrial depolarization, and morphological changes that take place during tumor necrosis factor (TNF)-α-induced cell death in HeLa cells. These reactions were analyzed at the single-cell level with 0.5 – 1 min resolution by using green fluorescent protein (GFP)-variant-derived probes and chemical probes. Cytochrome *c* release, caspase activation, and cellular shrinkage were always observed in this order within 10 min in all dying cells. This sequence of events was thus considered a critical pathway of cell death. Mitochondrial depolarization was also observed in all dying cells observed, but frequently occurred after caspase activation and cellular shrinkage. Mitochondrial depolarization is therefore likely to be a reaction that does not induce caspase activation and subsequent cellular shrinkage. Mitochondrial changes are important for apoptotic cell death; moreover, cytochrome *c* release, and not depolarization, is a key reaction related to cell death. In addition, we also found that the apoptotic pathway proceeds only when cells are exposed to TNF-α. These findings suggest that the entire cell death process proceeds rapidly during TNF-α exposure.

Keywords: tumor necrosis factor (TNF)-α, cytochrome *c*, mitochondrial depolarization, caspase, real-time imaging

Introduction

Apoptosis is a mechanism of cell death that is mediated by various intracellular reactions. A family of cysteine proteases, the caspases, forms the activation cascade, and these proteases play a central role in the apoptotic cell death machinery (1, 2). The caspases usually exist as pro-proteins in living cells and are activated by cleavage at the time when cell death is induced. In an early phase of the cell death process, initiator caspases are activated, which in turn activate effector caspases (3 – 7). Activated effector caspases cleave a number of different target proteins, and this cleavage leads ultimately to apoptotic cell death (8, 9). Mitochondria also play an important role in the cell death process (10 – 13). Cellular stresses induce mitochondrial changes, including an increase in outer mitochondrial membrane permeability; various mitochondrial proteins such as cytochrome *c* (cyt.*c*) and second mitochondrial activator of caspases (Smac) are released into the cytosol. Released proteins directly or indirectly regulate caspase activation and/or other reactions, which eventually induce cell death.

Various factors in the cell death process have been identified, but correlation among these factors remains unclear. Cell death events such as caspase activation and mitochondrial changes are rapid processes, and the onset of these events varies between individual cells (14 – 17). So, it is difficult to determine how and when such

*Corresponding author (affiliation #3). hkawai@jiu.ac.jp
#Present affiliation: Division of Drugs, National Institute of Health Sciences, Tokyo 158-8501, Japan
Published online in J-STAGE: February 8, 2007
doi: 10.1254/jphs.FP0060877

reactions occur in cells as based on analyses of cell populations, which can only be used to detect an average value for a large number of individual cells. In order to gain a better understanding of the cell death mechanism, simultaneous multi-events analyses should be conducted at the single-cell level and with high spatial and temporal resolution. Real-time imaging with confocal microscopy is a powerful method of detecting the manner in which such rapid intracellular reactions take place (18, 19).

Fluorescence resonance energy transfer (FRET) is useful for imaging analyses. Variants of green fluorescent protein (GFP) are currently widely employed; several families of fluorescent proteins have recently been reported to be useful for FRET analysis (19 – 22). Previously, we developed genetically-encoded sensors for caspase activation that consist of two fluorescent proteins linked by a small peptide (23, 24). Cyan-, green-, yellow-, and red-fluorescent proteins (CFP, GFP, YFP, DsRed) were used in combination as the fluorescent proteins. The small peptide was derived from a substrate of caspase, poly(ADP-ribose)polymerase; this fusion protein was primarily cleaved by caspase 3 (23). The sensor protein exhibits FRET in its intact form. However, in the presence of active caspase, the peptide is cleaved, and the two fluorescent proteins are rendered far apart; in this case, the sensor protein no longer exhibits any FRET. Caspase activation is detected as a reduction in FRET. We have previously reported that the use of various color combinations facilitates real-time imaging analysis. In particular, GFP-DsRed and YFP-DsRed have been shown to be as sensitive as CFP-YFP, which is commonly used as the FRET pair. FRET probes that consist of such color variations may be useful for simultaneous multi-event imaging (24).

In this study, we used the YFP-DsRed version of the effector-caspase sensor (YRec), CFP-tagged cyt.*c* (cyt.*c*-CFP), and tetramethylrhodamine methyl ester (TMRM) in order to detect caspase activation, cyt.*c* release from the mitochondria, and mitochondrial depolarization, respectively. By applying two of these probes simultaneously, two events could be monitored in the same cell, and the temporal relationships between caspase activation and mitochondrial changes could be examined at the single-cell level. In addition, we also analyzed the interval from tumor necrosis factor (TNF)-α exposure to cellular shrinkage by analyzing the cell population in order to investigate time course of the whole cell death process.

Materials and Methods

Plasmid construction

A plasmid encoding YRec, YFP-peptide-DsRed, was generated as previously reported (24). The sequence encoding the 11 amino acids at the C-terminus of YFP was eliminated in this construct. The C-terminal-truncated forms of the YFP gene were generated by PCR with primers containing the NheI site or the BspEI site and pEYFP-C1 (Clontech, Palo Alto, CA, USA) as a template, and the restricted fragment was inserted into the NheI/BspEI sites of pEYFP-C1 in order to generate a plasmid carrying truncated YFP. The oligonucleotides encoding the caspase's substrate sequence was inserted into the BspEI – AgeI site of the p(truncated YFP)-C1 vector to generate pYFP-PARP. The substrate sequence was derived from PARP (KRKGDEVDGVDE, 5'-CCGGAAAGAGAAAAGG CGATGAGGTGGATGGAGTGGATGAA-3' and 5'-CCGGTTCATCCACTCCATCCACCTCATCGCCTTT TCTCTTT-3'). DsRed was generated from pDsRed2-C1(Clontech) by PCR, at the AgeI/NotI sites, and the restricted fragment was inserted into the AgeI – NotI sites of pYFP-PARP to generate a plasmid carrying YFP-PARP-DsRed2 (YRec). YRec was cleaved by caspase-3 (23, 24).

Cyt.*c* was cloned from HeLa cells by RT-PCR with a primer pair (5'-TCGCTAGCGCTCCGGAGAATTAAA TATGGGTATG-3' and 5'-CGAGGATCCCTCATTAG TAGCTTTTTTGAG-3'), and the restricted fragment was inserted into the NheI – BamHI sites of the pECFP-N1 vector to generate a plasmid carrying cyt.*c*-CFP. All cloned sequences were verified by sequencing.

Cell culture and transfection

HeLa cells were cultured in DMEM (Sigma-Aldrich, St. Louis, MO, USA) supplemented with 100 units/ml of penicillin G, 100 μg/ml of streptomycin, and 10% fetal calf serum (GIBCO). The plasmid encoding the fluorescent probes was transfected into HeLa cells using Effectene Transfection Reagent (QIAGEN, Hilden, Germany) according to the manufacturer's instructions. After being incubated for 12 – 24 h with the transfection reagent, the cells were washed with PBS and cultivated on dishes suitable for an assay in medium containing 500 μg/ml of G418 for an additional 1 – 3 days until the assay was performed. We found that the cultivation period had no effect on cell death events after TNF-α treatment.

Bioimaging with fluorescence microscopy

Transfected cells were cultured on a cover glass (25-mm diameter, 0.15 – 0.18-mm thickness) for 1 – 3 days. Cells were treated with TNF-α (100 ng/ml, dissolved in PBS) and cycloheximide (10 μg/ml, dissolved in DMSO) and then were incubated under the usual culture conditions for 1 – 2 h prior to the analysis.

Table 1. Measurement conditions for real-time analysis by LSM510

Probe	Excitation (nm)	Beam splitter (nm)	Emission (nm)
Cyt.*c*-CFP	458	515	467.5 – 497.5
YRec	488	545	505 – 530 (donor)[a]
			560 – 615 (acceptor)[a]
TMRM	543	545	560 –[b]

[a]Emitted fluorescence was separated by a 545 dichroic mirror, and the fluorescence of the donor (YFP) and that of the acceptor (DsRed) was obtained via a band-pass emission filter. [b]A long-pass filter (LP560) was used.

Tetramethylrhodamine methyl ester (TMRM; 50 nM, dissolved in DMSO) was added to each sample 20 – 30 min prior to the analysis, when the mitochondrial membrane potential was to be measured (23, 25). Analyses were carried out by confocal laser scanning fluorescent microscopy using a Carl Zeiss LSM510 system (Carl Zeiss, Jena, Germany). During the observations, the media were buffered with 10 mM HEPES buffer (pH 7.4), and the cells were maintained at 35°C – 37°C. DIC images and grayscale images for fluorescence channels were obtained in 0.5- or 1-min intervals. Excitation lights for the cyt.*c*-CFP (458 nm) and YRec (488 nm) were provided by an Ar laser with a 458 or a 488 dichroic mirror, respectively. Excitation lights for the TMRM (543 nm) were provided by a HeNe laser with a 543 dichroic mirror. Images of the probes were obtained separately using a dichroic mirror and band-pass or long-pass emission filters, as indicated in Table 1. Contamination of the fluorescence between channels was negligible under these conditions (data not shown). For analyses involving YRec or TMRM, images were processed and quantified using MetaFluor software as follows: The average pixel intensity of the fluorescence of the entire cell region was determined for each channel. In the case of YRec, the ratio value was calculated as the average pixel value of the fluorescence ratio, (fluorescent intensity for the acceptor channel) /(fluorescent intensity for the donor channel), in the entire cell region. As the cells changed morphologically during the observation, the entire cell region was assessed separately for each image.

Simultaneous measurement of two probes was performed according to the multi-track scanning mode, in which two sets of excitation-detection conditions were used in alternation. For cyt.*c*-CFP and YRec, CFP fluorescence induced by excitation at 458 nm was measured in the first track, and YFP and DsRed fluorescence induced by excitation at 488 nm was measured in the second track. For cyt.*c*-CFP and TMRM, CFP fluorescence induced by excitation at 458 nm was measured in the first track, and TMRM fluorescence induced by excitation at 543 nm was measured in the second track. The scanning time difference between tracks was ca. 3 – 8 s, which was not significant in the temporal analysis.

Analysis of cell survival rate

HeLa cells were cultured in 96-well plastic plates to 80% – 90% confluency and were then treated with TNF-α. After the indicated culture durations, the cells were treated with Alamar Blue (Dainippon Pharmaceutical, Osaka) according to the manufacturer's instructions. Cell survival was measured as fluorescence at 590 nm induced by excitation at 540 nm. Fluorescence was measured using FlexStation (Molecular Devices, Sunnyvale, CA, USA).

Results

Simultaneous imaging of cyt.c-CFP and caspase sensor

HeLa cells expressing both cyt.*c*-CFP and YRec were treated with TNF-α, and changes in fluorescence were observed. Figure 1A shows DIC images, fluorescent images of CFP, and fluorescence ratio (DsRed/YFP) images of YRec during cell death. Images were obtained every 30 s; therefore, we were able to identify the time points of these events at a resolution period of 30 s. The CFP fluorescence indicated cyt.*c*-CFP localization, and the fluorescence ratio (DsRed/YFP) indicated caspase activation. CFP fluorescence was localized in the mitochondria at 280.5 min, and it was delocalized at 281.0 min, indicating that cyt.*c*-CFP was released during this period. The images shown in Fig. 1A indicate that this cell started to shrink at 286.5 – 287.0 min.

When the caspase was activated in a cell, the YRec was cleaved, which led to a reduction in the FRET from YFP to DsRed. Thus, a reduction in the fluorescence ratio (DsRed/YFP) reflected caspase activation. As shown in Fig. 1B, the fluorescence ratio decreased dramatically at 283.5 min in the cell shown here, thus indicating the initiation of caspase activation at this point in time. The increase in DsRed fluorescence

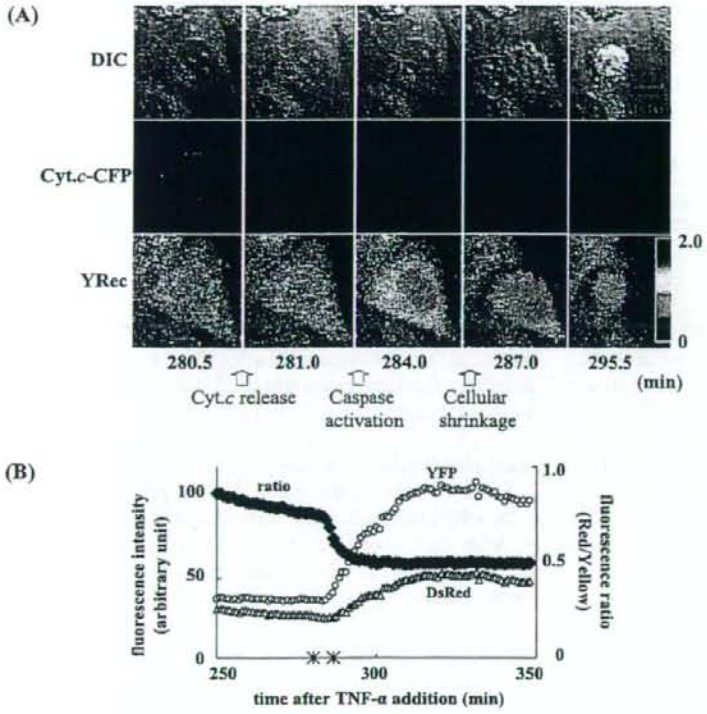

Fig. 1. Cyt.*c*-CFP release and caspase activation were monitored simultaneously in the same cells. A: DIC (upper), images showing the fluorescence of CFP (middle) and the fluorescence ratio of DsRed and YFP (DsRed /YFP, lower) during cell death are shown in pseudocolor. CFP and DsRed/YFP indicate the localization of cyt.*c*-CFP and caspase activation, respectively. B: Changes in YRec fluorescence in the cell shown in panel A were plotted. YFP and DsRed are shown with their fluorescence ratios. The asterisks indicate time points at which cyt.*c*-CFP were released and cell shrinkage was observed. The horizontal axis represents the point in time after the addition of TNF-α.

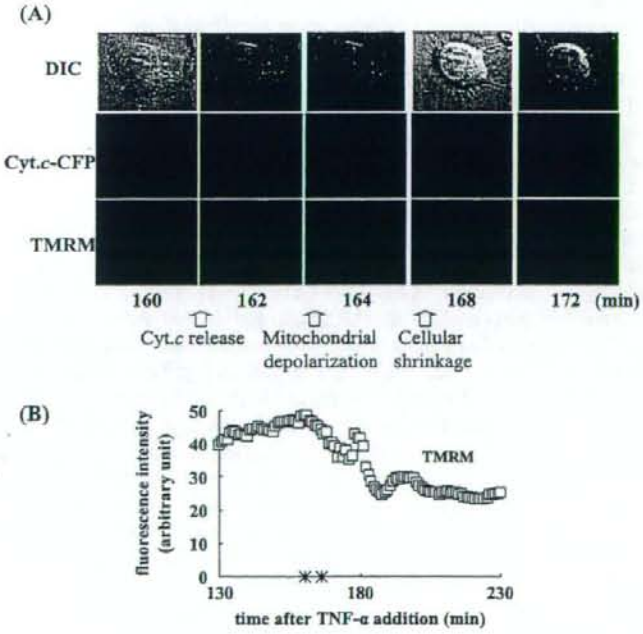

Fig. 2. Cyt.*c*-CFP release and mitochondrial depolarization were monitored simultaneously in the same cell. A: DIC (upper), images showing the fluorescence of CFP (middle) and the fluorescence of TMRM (lower) during cell death are shown in pseudocolor. CFP and TMRM fluorescence indicate the localization of cyt.*c*-CFP and the mitochondrial membrane potential, respectively. B: Changes in TMRM fluorescence of the cells in panel A during cell death were plotted. The asterisks indicate time points at which cyt.*c*-CFP were released and cell shrinkage was observed. The horizontal axis represents the point in time after the addition of TNF-α.

observed after this time point was unexpected, but is thought to have been the result of cellular shrinkage. Because the cell volume was reduced, the DsRed became concentrated, and the fluorescence increased. The reduction in the fluorescence ratio clearly indicated a reduction in FRET, which indicated both the cleavage of YRec as well as caspase activation. The asterisks indicate the time point of cyt.*c*-CFP release and cellular shrinkage, as determined based on the results shown in Fig. 1A. In this cell, cyt.*c*-CFP was released 280.5 min after the addition of TNF-α, and caspase activation was initiated 3 min after cyt.*c*-CFP release; the cell then started to shrink 3 min after caspase activation. Cyt.*c*-CFP release, caspase activation, and cellular shrinkage were observed in this order in all of the dying cells examined.

Simultaneous imaging of cyt.c-CFP and TMRM

HeLa cells expressing cyt.*c*-CFP were treated with TMRM and TNF-α. Delocalization of cyt.*c*-CFP and mitochondrial depolarization were observed with a resolution period of 1 min. All dying cells exhibited cyt.*c*-CFP release, mitochondrial depolarization, and shrinkage of the cell body. Figure 2A shows a typical fluorescent image of a dying cell. In this cell, cyt.*c*-CFP was released at 161 min, and cell shrinkage began at 167 min after the addition of TNF-α. Changes in TMRM fluorescence are plotted in Fig. 2B. TMRM fluorescence started to decrease at 164 min, thus indicating that the mitochondria started to depolarize at this point in time.

In a comparison of the starting points of these three events, it was found that the release of cyt.*c*-CFP always preceded mitochondrial depolarization and cellular shrinkage. Mitochondrial depolarization was observed earlier than cellular shrinkage in this particular cell, but was observed later in other cells. The temporal order of the timing of the initiation of mitochondrial depolarization and cellular shrinkage was not consistent. Mitochondrial depolarization preceded cellular shrinkage in 4 of the 10 cells, and cellular shrinkage preceded mitochondrial depolarization in 6 of the cells observed here.

Temporal relationships between mitochondrial changes, caspase activation, and cellular shrinkage

We observed 10 – 22 cells in each of these experiments, the results of which are shown in Figs. 1 and 2. We then determined the timing of cyt.*c* release, cellular shrinkage, and mitochondrial depolarization, or caspase activation in each cell. To clarify the temporal relationships between these cellular events, relative timing was

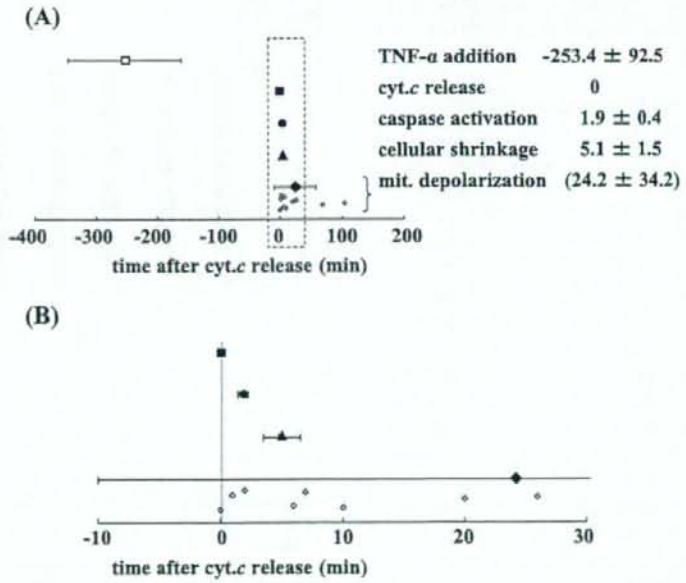

Fig. 3. Temporal relationship between mitochondrial changes and caspase activation. A: Relative timing of TNF-α addition (open square), cyt.*c* release (closed square), caspase activation (closed circle), cellular shrinkage (closed triangle), and mitochondrial depolarization (closed and open diamond) is shown with respect to time after cyt.*c* release. B: Shows a magnification of panel A.

determined as follows: the time point of cyt.*c* release was considered as time 0 in each of the individual cells. We calculated the relative timing of each of the observed events for each cell, and the results are plotted in Fig. 3. TNF-α treatment, cyt.*c* release, caspase activation, and cellular shrinkage are indicated as the mean ± S.D. Since mitochondrial depolarization did not give a normal distribution, all data for mitochondrial depolarization were plotted. Each plot represents the results from a single cell. Figure 3B shows magnification at around time 0.

The relative timing of TNF-α treatment and mitochondrial depolarization was found to deviate substantially, whereas the relative timing of caspase activation and cellular shrinkage gave only a small deviation. A substantial amount of time was required for the initiation of cyt.*c* release, and the duration varied between cells; however, after cyt.*c* release, the subsequent reactions occurred rapidly. After cyt.*c* release, cells are unable to stop or delay the cell death process.

Mitochondrial depolarization occurred before both caspase activation and cellular shrinkage in some of the cells (n = 4), but mitochondrial depolarization occurred after caspase activation and cellular shrinkage in other cells (n = 6). This finding suggests that mitochondrial depolarization is not necessary for either caspase activation or cellular shrinkage. Mitochondrial depolarization has been consistently reported as being associated with cell death, but it is not thought to be a critical step in the induction of apoptotic cell death.

Effects of the duration of TNF-α treatment

At the first step of TNF-α-induced cell death, TNF-α binds with its receptor on the cell surface, and an extracellular signal is transferred into the cell. After this step, Bid transfers the signal to the mitochondria, and then cyt.*c* is released from the mitochondria to the cytosol. Our results shown in Fig. 3 indicate that these processes took about 4 h. In order to analyze the timing of the onset of the earliest steps, we attempted to determine the point in time at which the first step started. To this end, we changed the duration of TNF-α exposure and measured the resulting cell survival rate. Cells were divided to two groups, as shown in Fig. 4A, and the cells were exposed to TNF-α for 0 – 12 h. In group A, the survival rate was measured immediately after TNF-α exposure. In group B, TNF-α was washed off after the indicated exposure time, and the cells were cultured in fresh medium without TNF-α for an additional 6 – 11 h, and the survival rate was then measured. If the cell death process proceeded after the removal of TNF-α, the survival rate would be expected to be reduced due to the additional culture period after the removal of TNF-α. In other words, more cells would be expected to have died in group B than in group A with the same amount of TNF-α exposure time.

The results showed that the survival rate decreased with increasing TNF-α exposure time (Fig. 4B). However, the survival rate did not decrease after TNF-α removal. This result suggests that the dead cells in group B had died during the period of TNF-α exposure, and that those cells that had survived during TNF-α exposure did not die after the removal of TNF-α. Thus, the cell death process is likely to proceed only when the cells were exposed to TNF-α. The survival rate in group B increased when cells were exposed TNF-α for 6 h. The biological meaning of this increase was unknown; however, this result did not disturb our conclusion.

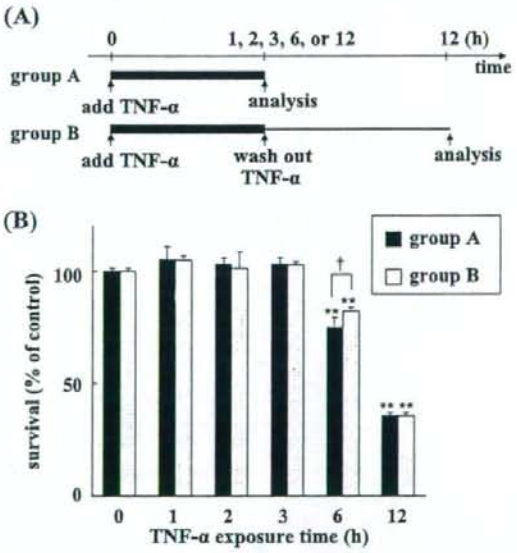

Fig. 4. Cell survival rate after TNF-α exposure. Panel A: Experimental design of the TNF-α exposure analysis. Thick lines represent the incubation in the presence of TNF-α, and thin line represents the incubation in the absence of TNF-α. In group A, cells were exposed to TNF-α for the indicated amount of time, and the cell survival rate was measured immediately. In group B, cells were exposed in the same manner as that used for group A. Then, the TNF-α was washed out, and the cells were cultured in fresh media for 6 – 11 h. Then, the cell survival rate was measured. The total duration of the culture period after the onset of TNF-α exposure was 12 h in group B. Panel B: The cells in groups A and B were exposed to TNF-α for 1, 2, 3, 6, or 12 h, and the cell survival rates were determined. Each bar represents a mean ± S.D. (n = 6). $^{**}P<0.01$ *vs* time 0, according to Dunnett's test. $^{\dagger}P<0.05$ between groups A and B, according to Student's *t*-test.

Discussion

This is the first report to reveal the precise temporal relationships between four reactions (mitochondrial depolarization, cyt.*c* release, caspase activation, and cellular shrinkage) in TNF-α-induced cell death. Because the onset of these reactions varied among individual cells, real-time single-cell imaging is the only currently available method to reveal temporal relationships between these reactions. We described our three-color real-time imaging technique in this report. Rehm et al. has reported the simultaneous real-time imaging of caspase activation and Smac release by using CFP/YFP-FRET sensor and YFP-tagged protein (26). They used the same color, YFP, for the observation of both reactions. It is possible to identify two reactions as they discussed, but it may be difficult to identify small changes occurring in the cell by their method. Previously, we revealed that DsRed was useful for FRET analysis of caspase activation (24). In this report, we observed caspase activation and cyt.*c* release with YFP/DsRed-FRET sensor and CFP-tagged protein. By using fluorescent probes in different colors, each reaction could be easily and precisely identified in a single cell.

We observed cell death at the single-cell level with a resolution period of 0.5 – 1 min, and we revealed that the relative timing between cyt.*c* release, caspase activation, and cellular shrinkage remained constant in all of the dying cells observed; however, the timing of mitochondrial depolarization showed a large deviation (Fig. 3). After cyt.*c* release, apoptosome formation, caspase-9 activation, caspase-3 activation, and the cleavage of various substrates that lead to apoptotic cell death are initiated. Our results revealed that this series of reactions takes place within 10 min and that the time course of this process was identical among all of the dying HeLa cells.

Mitochondrial depolarization was observed in all dying cells, but we considered that mitochondrial depolarization was not the cause of cyt.*c* release, caspase activation, and cellular shrinkage. Mitochondrial depolarization was found to occur at any time after cyt.*c* release. Mitochondrial depolarization was observed after caspase activation and cellular shrinkage in 60% of the observed cells. These results exclude the possibility that mitochondrial depolarization is a cause of cyt.*c* release, caspase activation, and/or cellular shrinkage. This is consistent with previous findings that cell death occurred without mitochondrial depolarization. Li et al. have shown that caspases are activated independently of mitochondrial depolarization in TNF-α-induced cell death (27). Krohn et al. have shown that cyt.*c* release and caspase activation occurred in the absence of mitochondrial depolarization in cell death of hippocampal neurons (28). Several studies suggested that mitochondrial depolarization is a critical step for cell death (29), but our results support the idea that mitochondrial depolarization is not crucial to the cell death process.

Cyt.*c* release may be a key step in two independent series of events, that is, the cell death process and mitochondrial depolarization. We speculate that cells might try to maintain cellular homeostasis by keeping membrane potential after cyt.*c* release. While maintaining the membrane potential, the released cyt.*c* immediately initiated the cell death process in the cytosol, and thus caspase activation and cellular shrinkage always took place within a short period of time. The timing of mitochondrial depolarization did not appear to be relevant to this process.

A number of imaging analyses have demonstrated that each cell death event is a rapid process. Initiator- and effector-caspase activation both proceed rapidly (23, 24, 30 – 32). Cyt.*c* is also released rapidly in a single step (33 – 35). Likewise, Smac/DIABLO is released rapidly, although the duration of Smac/DIABLO release is greater than that of cyt.*c* (26). Several multi-event imaging studies have suggested that cell death events occur almost simultaneously. Initiator caspase activation/effector caspase activation, effector caspase activation/mitochondrial depolarization, cyt.*c*/smac, and effector caspase activation/smac release had been analyzed simultaneously at the single-cell level and were found to occur almost simultaneously (24, 26). These findings, taken together with our present results, suggest that the cell death cascade proceeds rapidly after mitochondrial changes take place.

Once cyt.*c* was released, the following reactions proceed in a rapid manner. However, it did take 253.4 ± 92.5 min from TNF-α treatment to cyt.*c* release, and this duration varied from cell to cell (Figs. 3 and 4). We observed some cells that had died within 1 h in imaging analysis, indicating that cells have the ability to induce cell death within 1 h, and suggesting that certain factors may delay signal transduction and the timing of cell death. The results shown in Fig. 4 indicate that these factors were active only when the cells were exposed to TNF-α. We considered two possible explanations for these findings. 1: Each TNF-α molecule changed the cell slightly, and the changes induced by one molecule were not sufficient to induce the cell death cascade on their own. However, many TNF-α molecules attacked the cell, and intracellular changes thus accumulated. When the accumulated changes exceeded the threshold level, the cell death cascade would be expected to have

proceeded rapidly. 2: TNF-α could induce intracellular changes by chance. According to this explanation, TNF-α molecules would bind with the TNF receptor, but only some of them would be able to induce intracellular change. If some TNF-α molecules successfully induce intracellular changes, then the cell death cascade would proceed rapidly. The more TNF-α molecules that are present around the cell, and/or the longer these TNF-α molecules attack the cell, the higher the probability of a successful attack, and it can be expected that more cells will die. According to both of these models, the cell death process would not proceed in the absence of TNF-α exposure; therefore, those cells that survived during TNF-α exposure would not be expected to die after the removal of TNF-α.

One of the Bcl-2 family proteins, Bid, was cleaved to tBid due to the cell death signal, and the tBid transferred the signal from the cytosol to the mitochondria (36). Exogenous treatment with tBid is known to induce cell death immediately (37), and thus reactions that delay signal transduction may occur at an earlier step than either Bid cleavage or mitochondrial changes.

As cell death reactions often occur in a rapid manner and because the timing of the onset of intracellular reactions varies among cells, precise temporal relationships between cellular events during cell death should be further analyzed at the single-cell level with high temporal resolution. Single-cell imaging analyses of early stages (e.g., receptor oligomerization and the recruitment of adaptor proteins) will help to elucidate the mechanism of the entire cell death process.

Acknowledgments

This study was supported in part by a Grant-in-Aid for Research on Health Sciences focusing on Drug Innovation from the Japan Health Science Foundation; a Grant-in-Aid for Research on Advanced Medical Technology from the Ministry of Health, Labour, and Welfare; and a grant (MF-16) from the Organization for Pharmaceutical Safety and Research.

References

1 Thornberry NA, Lazebnik Y. Caspases: enemies within. Science. 1998;281:1312–1316.
2 Stennicke HR, Salvesen GS. Properties of caspases. Biochim Biophys Acta. 1998;1387:17–31.
3 Boldin MP, Goncharov TM, Goltsev YV, Wallach D. Involvement of MACH, a novel MORT1/FADD-interacting protease, in Fas/APO-1- and TNF receptor-induced cell death. Cell. 1996; 85:803–815.
4 Muzio M, Chinnaiyan AM, Kischkell FC, O'Rourke K, Shevchenko A, Ni J, et al. FLICE, a novel FADD-homologous ICE/CED-3-like protease, is recruited to the CD95 (Fas/APO-1) death-inducing signal complex. Cell. 1996;85:817–827.
5 Medema JP, Scaffidi C, Kischkel FC, Shevchenko A, Mann M, Krammer PH, et al. FLICE is activated by association with the CD95 death-inducing signaling complex (DISC). EMBO J. 1997;16:2794–2804.
6 Martin DA, Siegel RM, Zheng L, Lenardo MJ. Membrane oligomerization and cleavage activates the caspase-8 (FLICE /MACHalpha1) death signal. J Biol Chem. 1998;273:4345–4349.
7 Srinivasula SM, Ahmad M, Fernandes-Alnemri T, Litwack G, Alnemri ES. Molecular ordering of the Fas-apoptotic pathway: The Fas/APO-1 protease Mch5 is a CrmA-inhibitable protease that activates multiple Ced-3/ICE-like cysteine proteases. Proc Natl Acad Sci U S A. 1996;93:14486–14491.
8 Orth K, O'Rourke K, Salvesen GS, Dixit VM. Molecular ordering of apoptotic mammalian CED-3/ICE-like proteases. J Biol Chem. 1996;271:20977–20980.
9 Tewari M, Quan LT, O'Rourke K, Desnoyers S, Zeng Z, Beidler DR, et al. Yama/CPP32 beta, a mammalian homolog of CED-3, is a CrmA-inhibitable protease that cleaves the death substrate poly(ADP-ribose) polymerase. Cell. 1995;81:801–809.
10 Green DR, Reed JC. Mitochondria and apoptosis. Science. 1998;281:1309–1312.
11 Martinou JC, Green DR. Breaking the mitochondrial barrier. Nat Rev Mol Cell Biol. 2001;2:63–67.
12 Saleh A, Srinivasula SM, Acharya S, Fishel R, Alnemri ES. Cytochrome c and dATP-mediated oligomerization of Apaf-1 is a prerequisite for procaspase-9 activation. J Biol Chem. 1999;274:17941–17945.
13 Shiozaki EN, Chai J, Shi Y. Oligomerization and activation of caspase-9, induced by Apaf-1 CARD. Proc Natl Acad Sci U S A. 2002;99:4197–4202.
14 Tyas L, Brophy VA, Pope A, Rivett AJ, Tavare JM. Rapid caspase-3 activation during apoptosis revealed using fluorescence-resonance energy transfer. EMBO reports. 2000;1:266–270.
15 Rehm M, Dussmann H, Janicke RU, Tavare JM, Kogel D, Prehn JHM. Single-cell fluorescence resonance energy transfer analysis demonstrates that caspase activation during apoptosis is a rapid process: role of caspase-3. J Biol Chem. 2002;277: 24506–24514.
16 Luo KQ, Yu VC, Pu Y, Chang DC. Application of the fluorescence resonance energy transfer method for studying the dynamics of caspase-3 activation during UV-induced apoptosis in living HeLa cells. Biochem Biophys Res Commun. 2001;283:1054–1060.
17 Morgan MJ, Thorburn A. Measurement of caspase activity in individual cells reveals differences in the kinetics of caspase activation between cells. Cell Death Differ. 2001;8:38–43.
18 Tsien RY, Miyawaki A. Seeing the machinery of live cells. Science. 1998;280:1954–1955.
19 Miyawaki A, Sawano A, Kogure T. Lighting up cells: labeling proteins with fluorophores. Nat Cell Biol. 2003;S1–S7.
20 Tsien RY, The green fluorescent protein. Annu Rev Biochem. 1998;67:509–544.
21 Erickson MG, Moon DL, Yue DT. DsRed as a potential FRET partner with CFP and GFP. Biophys J. 2003;85:599–611.
22 Karasawa S, Araki T, Nagai T, Mizuno H, Miyawaki A. Cyan-emitting and orange-emitting fluorescent proteins as a donor

/acceptor pair for fluorescence resonance energy transfer. Biochem J. 2004;381:307–312.
23 Kawai H, Suzuki T, Kobayashi T, Mizuguchi H, Hayakawa T, Kawanishi T. Simultaneous imaging of initiator / effector caspase activity and mitochondrial membrane potential during cell death in living HeLa cells. Biochim Biophys Acta. 2004;1693:101–110.
24 Kawai H, Suzuki T, Kobayashi T, Sakurai H, Ohata H, Honda K, et al. Simultaneous real-time detection of initiator- and effector-caspase activation by double fluorescence resonance energy transfer analysis. J Pharmacol Sci. 2005;97:361–368.
25 Scaduto RC Jr, Grotyohann LW. Measurement of mitochondrial membrane potential using fluorescent rhodamine derivatives. Biophys J. 1999;76:469–477.
26 Rehm M, Dussmann H, Prehn JHM. Real-time single cell analysis of Smac/DIABLO release during apoptosis. J Cell Biol. 2003;162:1031–1043.
27 Li X, Du L, Darzynkiewicz Z. During apoptosis of HL-60 and U-937 cells caspases are activated independently of dissipation of mitochondrial electrochemical potential. Exp Cell Res. 2000;257:290–297.
28 Krohn AJ, Wahlbrink T, Prehn JHM. Mitochondrial depolarization is not required for neuronal apoptosis. J Neurosci. 1999;19:7394–7404.
29 Heiskanen KM, Bhat MB, Wang H-W, Ma J, Nieminen A-L. Mitochondrial depolarization accompanies cytochrome c release during apoptosis in PC6 cells. J Biol Chem. 1999;274:5654–5658.
30 Ohnuki R, Nagasaki A, Kawasaki H, Baba T, Uyeda TQP, Taira K. Confirmation by FRET in individual living cells of the absence of significant amyloid β-mediated caspase 8 activation. Proc Natl Acad Sci U S A. 2002;99:14716–14721.
31 Takemoto K, Nagai T, Miyawaki A, Miura M. Spatio-temporal activation of caspase revealed by indicator that is insensitive to environmental effects. J Cell Biol. 2003;160:235–243.
32 Luo KQ, Yu VC, Pu Y, Chang DC. Measuring dynamics of caspase-8 activation in a single living HeLa cell during TNFalpha-induced apoptosis. Biochem Biophys Res Commun. 2003;304:217–222.
33 Lim MLR, Lum M-G, Hansen TM, Roucou X, Nagley P. On the release of cytochrome c from mitochondria during cell death signaling. J Biomed Sci. 2002;9:488–506.
34 Goldstein JC, Waterhouse NJ, Juin P, Evan GI, Green DR. The coordinate release of cytochrome c during apoptosis is rapid, complete and kinetically invariant. Nat Cell Biol. 2000;2:156–162.
35 Goldstein JC, Munoz-Pinedo C, Ricci J-E, Adams SR, Kelekar A, Schuler M, et al. Cytochrome c is released in a single step during apoptosis. Cell Death Differ. 2005;12:453–462.
36 Luo X, Budihardjo I, Zou H, Slaughter C, Wang X. Bid, a Bcl-2 interacting protein, mediates cytochrome c release from mitochondria in response to activation of cell surface death receptors. Cell. 1998;94:481–490.
37 Madesh M, Antonsson B, Srinivasula SM, Alnemri ES, Hajnóczky G. Rapid kinetics of tbid-induced cytochrome c and Smac/DIABLO release and mitochondrial depolarization. J Biol Chem. 2002;277:5651–5659.

Available online at www.sciencedirect.com
SCIENCE DIRECT
Biologicals 34 (2006) 65–68
IABs BIOLOGICALS
www.elsevier.com/locate/biologicals

Regulatory perspectives from Japan — Comparability of biopharmaceuticals☆

Toru Kawanishi*

Division of Biological Chemistry and Biologicals, National Institute of Health Sciences, 1-18-1 Kamiyoga, Setagaya-ku, Tokyo 158-8501, Japan

Accepted 22 August 2005

Abstract

In Japan there is no official guideline about comparability assessment of biotechnological products at present. However, there is some notifications which should be referred to, when the manufacturer changes the manufacturing process. Here, regulatory perspectives from Japan on the comparability assessment are presented. When establishing the comparability of biotechnological products derived from different manufacturing processes and the validity of modified manufacturing process, rational step-by-step approaches based on both product and process aspects would be useful. At first, relevant physicochemical and biological properties of products including purity, impurity profiles and stability should be compared before and after the manufacturing change, depending on the type and nature of the desired products. It is also necessary to examine the capacities of the new manufacturing process for ensuring the consistent production of the active protein product as well as the anticipated elimination of potential impurities and contaminants. Further relevant assessment of preclinical and clinical comparability of product may be necessary in some cases.

Keywords: Biotechnological product; Comparability; Japan; ICH-guideline; Regulatory perspectives; Harmonization

1. Introduction

Biotechnological products were developed and produced based on many innovative technologies, which are always advancing by themselves. The products are, therefore, often subject to change in the manufacturing process for improvement of the product quality and production economy, increase in production yield, and so on. It is not reasonable that the manufacturers are required to submit the same full data to obtain the authorization of the manufacturing change as to obtain the new drug authorization. USA-FDA and EU-CPMA have already set each guideline for comparability assessment of biotechnological/biological products. We had also started the discussion about the comparability guideline in Japan. However, we stopped developing it, because comparability assessment of biotechnological products was nominated as a candidate of the new topic in the ICH-Quality. Drafting of the harmonized guideline has just started in the ICH-EWG. Here, I would like to give the regulatory perspectives about the comparability assessment of biopharmaceuticals from Japan.

2. Present official notifications relating with comparability assessment of biotechnological products before and after manufacturing changes in Japan

In Japan, we do not have any official guideline for the comparability assessment of biotechnological/biological products whose manufacturing processes are changed, yet. However, there is a notification, which should be referred to, when the manufacturer changes the manufacturing process of biotechnology-derived drugs which have already been approved. That is the Notification No. 243 from the Pharmaceutical Affairs Bureau, MHW of 1984. However, nearly 20 years have already passed since the Notification was made and some parts

☆ The perspectives are before the discussion in the ICH-EWG.

* Tel./fax: +81 3 3700 9064.
E-mail address: kawanish@nihs.go.jp

1045-1056/06/$32.00
doi:10.1016/j.biologicals.2005.08.017

of the requirement are assumed to be too strict. At present we usually treat each case as summarized below.

The following recombinant drugs would be treated as "not new drugs", which are categorized as "1-(8) other drugs" in the Pharmaceutical Affairs Bureau Notification No. 698: the first is the product which contains identical active ingredient although the culture method is different from the approved drug; the second is that which contains identical active ingredient although the purification process is different from the approved drug; and the third is the other drug in which difference is not specified. The followings are also usually treated as "not new drugs" but decided on a case-by-case basis: the product which contains identical active ingredient but its structure gene is identified by different process; and the product which contains identical active ingredient but host cell/vector system is different from the approved drug. In the case of the category 1-(8) other drugs as "not new drug", the data on specification and test methods, stability, and bioequivalence are required to be submitted for the registration as the pharmaceuticals, and a list of literature references concerning toxicity, pharmacological action, absorption, distribution, metabolism and excretion, and clinical trials for active ingredients concerned, as well as an outline of the list contents and the results of evaluation test are also required. In addition, in the case of the biotechnology-derived drugs, the following data are also needed on a case-by-case basis:

data on the manufacturing process, physicochemical analysis, specifications and test methods, stability;
data on single dose administration toxicity in one species of animals;
data on bioequivalency study;
data on clinical study for safety, etc.

The present notifications relating with the comparability of the products between before and after the changes in the manufacturing process in Japan are very simple, as summarized above. However, we have discussed much how to assess comparability of biotechnological products to draft the guideline, within Japanese experts. The following is the perspectives obtained from the discussion.

3. Regulatory perspectives from Japan: "how should we assess comparability of biotechnological products before and after the manufacturing change?"

To date, various topics related to the characterization and quality assessment as well as the manufacturing process for biotechnological products have been the subject of ICH harmonized guidelines and have proven very useful, in allowing manufacturers to develop a global approach to these issues. However, there is no specific international guideline on comparability of biotechnological products subject to changes in the manufacturing process. The subject we are facing is how to develop and establish rational concepts and approaches for establishing comparability of protein products derived from different biopharmaceutical manufacturing processes.

3.1. When is comparability assessment needed?

A comparability assessment is needed when a manufacturer wants to claim that the product of new manufacturing process Y is comparable to the already existing product of manufacturing process X with respect to quality, safety and efficacy (Fig. 1). The new process Y would be employed by either the same manufacturer, innovator or by different subsequent-entry manufacturer(s). The existing product from process X may be either an already licensed one or one under development for new drug application for approval. In case where there is an already licensed drug, subsequent-entry product(s) from different manufacturer(s) will be dealt with as a so-called generic product(s). On the other hand, the application from the innovator will be handled as a partial variation from already licensed conditions for the drug with respect to the manufacturing process. In the case of manufacturing variation of the product under development, the issue becomes the verification of such change within a single manufacturer at various stages of product development from early stage research to pre-approval. Here, the followings should be mentioned: it has been already decided that the generic products are excluded from the scope of the ICH-Q5E comparability guideline, but in Japan we still think that the comparability of the generic products could be evaluated following the same scientific approach.

3.2. General principles of comparability assessment

When establishing the comparability of biotechnological products derived from different manufacturing processes and the validity of modified manufacturing process, rational step-by-step approaches based on both product and process aspects would be useful. In this approach, the following parameters should be considered as key points:

(1) physicochemical and biological characterizations;
(2) impurities profile and the presence of potential contaminants;
(3) batch analysis;
(4) product stability;
(5) manufacturing process evaluation/validation studies; and in wider perspective
(6) preclinical and clinical studies.

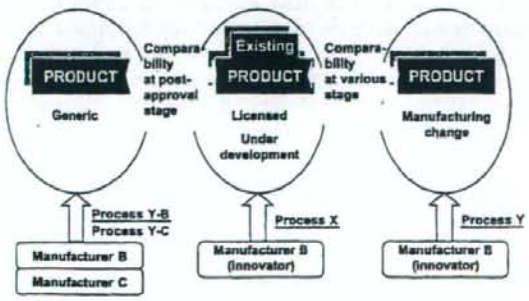

Fig. 1. Various cases of comparability assessment.

3.3. Strategies for comparability assessment

From the viewpoint of product aspects, the essential and critical first step is to establish whether the new candidate product in question is comparable to the existing product in terms of molecular and quality attributes. This is because whatever changes (minor or major) in the manufacturing process are made, if the new candidate product in question is not comparable to the existing product in terms of molecular and quality attributes, the new one will rather be regarded as a novel molecular entity for new drug application, but not as a qualified candidate for further comparability studies. The candidate product should be, therefore, the subject of extensive identification and characterization, as well as quality assessments including tests on impurities profile and the presence of potential contaminants. If these attributes of the candidate product and process are found to be comparable to those of the previous ones, further assessment of preclinical and clinical comparability would be performed, where necessary and appropriate.

3.4. Comparability from product aspects

Before going into some details about the need for further assessment of preclinical and clinical comparability, however, one should ask the following key question: "what is the identity or comparability of the biosynthetic protein product which possesses the inherent degree of structural heterogeneity?" In other words, what kind of criteria should be applied for establishing the identity or comparability of the candidate product(s) compared to the previous product with respect to molecular and quality attributes?

To answer this question, we should remind new concepts in the ICH-Q6B document. In the document we have introduced the concept, which has defined the desired product and variants, so that an inherent degree of structural and quality heterogeneity can be dealt within a relevant way. Desired product is defined as: (1) the protein which has the expected structure, or (2) the protein which is expected from the DNA sequence and anticipated post-translational modification (including glyco-forms), and from the intended downstream modification to produce an active biological molecule. When molecular variants of the desired product are formed during manufacture and/or storage and have properties comparable to the desired product, they are considered to be product-related substances and incorporated into active ingredient. When molecular variants of the desired product do not have properties comparable to those of the desired product, they are considered to be product-related impurities. In the concept, active ingredient may be composed of the desired product and multiple product-related substances; the desired product can be a mixture of several molecular entities derived from anticipated post-translational modification. Impurities may be either process-related or product-related (Fig. 2).

Various cases are considered for minimum qualification for further comparability assessments depending on each following specific type of desired product (A–D):

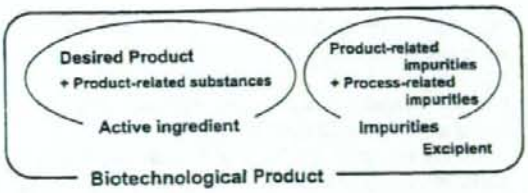

Fig. 2. New concept about biotechnological product in the ICH-Q6B.

(A) the protein which has the expected structure (e.g., monoclonal antibodies);
(B) the protein which is expected from the DNA sequence (simple protein);
(C) the protein which is expected from the DNA sequence and anticipated post-translational modification; and
(D) the protein which is expected from the intended downstream modification to produce an active biological molecule.

In the case of the "Desired product" being defined as the protein which has the expected structure, like monoclonal antibodies, minimum qualification for a candidate product for further comparability assessments should be that the product is derived from the same initial cell clone as a previous one and has comparable molecular and quality attributes compared to a previous one with respect to: (1) structural features, (2) physicochemical, (3) immunological properties, and (4) impurities profile. Variation of carbohydrate heterogeneity due to changes in culture conditions should be considered on a case-by-case basis.

In the case of the "Desired product" being defined as the protein which is expected from the DNA sequence, like recombinant insulin, minimum qualification for a candidate (product) for further comparability assessments should be that the product is the same as an already existing one with respect to protein structure, physicochemical and biological properties, as well as comparable impurities profiles.

In cases where the in vivo biological activity is closely related to the intended clinical effectiveness, further preclinical and clinical assessments with respect to efficacy may be omitted.

In the case of the "Desired product" being defined as the protein which is expected from the DNA sequence structure and anticipated post-translational modification, typically like glycoproteins, minimum qualification for a candidate product for further comparability assessments should be that the product is derived from the same initial cell clone as a previous product and has the same protein structure, comparable physicochemical properties, comparable carbohydrate patterns compared to a previous product with respect to the types of sialic acids and their contents, and antennary profile. Here, comparable biological properties, especially ensuring higher-order structure, in vivo activity and representing the clinical effectiveness, if any, is a critical factor for the qualification.

In the case of the protein which is expected from the intended downstream modification to produce an active

biological molecule, qualification for further comparability assessment of this type of products should be considered as a case-by-case issue, taking into account of types of modification and process change. Where necessary and appropriate, manufacturers should refer to the above cases A–C.

In this way, each specific type of candidate product can be qualified to be comparable to the pre-existing product with respect to molecular and quality attributes including impurity profile. The quality and extent of data obtained from studies on the molecular and quality attributes of the candidate would become one of the crucial elements for determining the necessity and extent of further comparability assessments, as well as for establishing the entire comparability to the pre-existing product.

3.5. Comparability from process aspect

As another aspect of quality comparability assessments, it is necessary to examine the capacities of a new manufacturing process for ensuring the consistent production of the active protein product as well as the anticipated elimination of potential impurities and contaminants. The capacities of the new process should not be less potent than those of the old process.

Changes in the manufacturing process used to make a particular product can be made in a variety of stages or steps of the process. Examples of such changes include: (1) method for generating cell substrate; (2) cell culture methods; (3) isolation and purification procedure; and (4) final product formulation. For changes in a certain stage of manufacturing process including cell substrate matters, relevant and complementary use of the ICH-guidelines (Q5A, Q5B, Q5EC, 5D, Q6B, and S6) would be encouraged.

Whatever changes in the manufacturing process are made, the effects of the changes, both direct and indirect, on the consistent production of the product should be considered and the modified process should be re-evaluated or re-validated as needed. The appropriate process re-evaluation or re-validation programs and criteria will vary depending on the nature and extent of the change. According to the results of process re-evaluation/re-validation studies on the new process, sometimes applicants may need to modify in-process controls including in-process testing and specifications of critical intermediates or final product (Fig. 3). The applicant should provide justification of such modification, if any.

3.6. Suitability of analytical method

As another dimension to comparability study, it is necessary to consider suitability of available analytical methods. Manufacturers should provide assurance that an appropriate set of analytical methods has been selected in order to assess the comparability of the product and to what extent the analytical methods used are suitable for comparability studies. The validation of the analytical methods used should be appropriate.

New analytical technology and modifications to existing technology are continually being developed and should be utilized when appropriate.

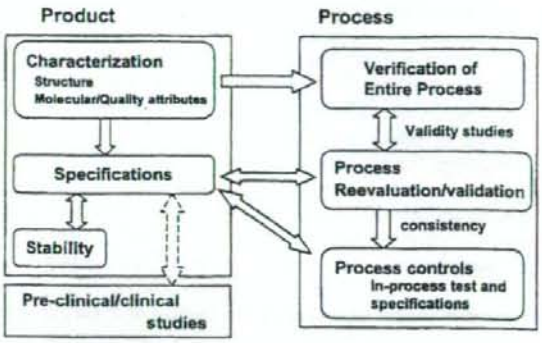

Fig. 3. Elements for ensuring product quality and consistency.

3.7. Preclinical and clinical studies

Further relevant assessment of preclinical and clinical comparability of product may be necessary, when it cannot be determined if the pre-existing product and the candidate product are comparable or not from the quality studies. The extent and nature of preclinical and clinical studies should be determined on a case-by-case basis in consideration of various factors. These include the followings:

- the nature of the product;
- intended clinical use;
- the extent of comparability of the candidate product to the existing counterpart with respect to molecular and quality attributes including impurity profile;
- the nature and extent of changes in manufacturing process;
- the results of the evaluation/validation studies on the new process including the results of relevant in-process tests;
- the capabilities and limitations of tests used for any comparability study;
- availability of existing preclinical and clinical data;
- the extent of existing information and experiences pertaining to the product in question; and
- stage of the product development.

Available online at www.sciencedirect.com
SCIENCE DIRECT®
Phytomedicine 13 (2006) 401–411
Phytomedicine
www.elsevier.de/phymed

Screening of novel nuclear receptor agonists by a convenient reporter gene assay system using green fluorescent protein derivatives

T. Suzuki[a,b], T. Nishimaki-Mogami[a], H. Kawai[a], T. Kobayashi[a], Y. Shinozaki[a], Y. Sato[a], T. Hashimoto[c], Y. Asakawa[c], K. Inoue[a], Y. Ohno[a], T. Hayakawa[a], T. Kawanishi[a,*]

[a] *National Institute of Health Sciences, Tokyo, Japan*
[b] *Pharmaceuticals and Medical Device Agency, Tokyo, Japan*
[c] *Faculty of Pharmaceutical Sciences, Tokushima Bunri University, Tokushima, Japan*

Received 27 September 2004; accepted 6 April 2005

Abstract

Nuclear receptors represent a very good family of protein targets for the prevention and treatment of diverse diseases. In this study, we screened natural compounds and their derivatives, and discovered ligands for the retinoic acid receptors (RARs) and the farnesoid X receptor (FXR). In the reporter assay systems of nuclear receptors presented here, two fluorescent proteins, enhanced yellow fluorescent protein (EYFP) and enhanced cyan fluorescent protein (ECFP), were used for detection of a ligand-based induction and as an internal control, respectively. By optimizing the conditions (e.g., of hormone response elements and promoter genes for reporter plasmids), we established a battery of assay systems for ligands of RARs, retinoid X receptor (RXR) and FXR. The screening using the reporter assay system can be carried out without the addition of co-factors or substrates. As a result of screening of more than 140 compounds, several compounds were detected which activate RARs and/or FXR. Caffeic acid phenylethyl ester (CAPE), known as a component of propolis from honeybee hives, and other derivatives of caffeic acid up-regulated the expression of reporter gene for RARs. Grifolin and ginkgolic acids, which are non-steroidal skeleton compounds purified from mushroom or ginkgo leaves, up-regulated the expression of the reporter gene for FXR.

Keywords: FXR; RAR; Reporter assay; Fluorescence; GFP; Caffeic acid; Ginkgolic acid; Grifolin

Introduction

Nuclear hormone receptors are ligand-activated transcription factors that are involved in a variety of physiological, developmental, and toxicological processes. The nuclear hormone receptor superfamily includes receptors for thyroid and steroid hormones, retinoids and vitamin D, as well as receptors for unknown ligands. These receptors share a highly conserved DNA-binding domain and a discrete ligand-binding domain, and bind to hormone response elements (HREs) on the DNA during the formation of homodimers, heterodimers, or monomers. This ligand binding to nuclear receptors leads to conformational

*Corresponding author. Tel.: +81 3 3700 9064; fax: +81 3 3700 9084.
E-mail address: kawanish@nihs.go.jp (T. Kawanishi).

0944-7113/$ - see front matter © 2005 Elsevier GmbH. All rights reserved.
doi:10.1016/j.phymed.2005.09.003

change of these receptors and the recruitment of coactivator complexes, resulting in transcriptional activation (Khorasanizadeh and Rastinejad, 2001). Their ligand-dependent activity makes nuclear receptors good pharmacological targets.

Nuclear receptors form a superfamily of phylogenetically related proteins encoded by 48 genes in the human genome. Three isotypes of retinoic acid receptors (RARs: RARα, RARβ and RARγ) are receptors for retinoids such as all-*trans*-retinoic acid (ATRA) (Petkovich et al., 1987; Brand et al., 1988; Krust et al., 1989). RARα is associated with differentiation therapy for human acute promyelocytic leukemia (Hansen et al., 2000). RARβ plays a central role in limiting the growth of different cell types (reviewed in Hansen et al., 2000), and is thus a possible target for the treatment of breast and other cancers. RARγ is also primarily expressed in the skin and is involved in skin photoaging and carcinogenesis, and in skin diseases such as psoriasis and acne (Fisher et al., 1996).

The farnesoid X receptor (FXR) is a receptor for bile acids such as chenodeoxycholic acid (CDCA), deoxycholic acid, cholic acid, and their conjugates. Bile acids are synthesized in the liver and secreted into the intestine, where their physical properties facilitate the absorption of fats and vitamins through micelle formation. Cholesterol disposal from the liver is also dependent on the bile acid composition of the secreted bile. Bile acids bind to FXR to activate and regulate the transcription of FXR target genes. FXR controls the expression of critical genes in bile acid and cholesterol homeostasis (Makishima et al., 1999; Parks et al., 1999; Wang et al., 1999). FXR-null mice show elevated serum cholesterol and triglyceride levels (Sinal et al., 2000), and an FXR agonist has been shown to reduce serum triglyceride levels (Maloney et al., 2000). FXR is thus an attractive pharmacological target for the treatment of hyperlipidemia. Moreover, an FXR agonist has been reported to confer hepatoprotection in a rat model of cholestasis (Liu et al., 2003).

The retinoid X receptor (RXR) is a common heterodimeric partner for many receptors, including thyroid hormone receptor (TR), RAR, vitamin D_3 receptor (VDR), peroxisome proliferator-activated receptor (PPAR), liver X receptor (LXR), and FXR, in addition to functioning as a receptor for 9-*cis*-retinoic acid (9CRA) during formation of a homodimer.

To determine ligands for these nuclear receptors, we developed a reporter assay system using GFP derivatives. To study the promoter and enhancer control of gene expression, firefly luciferase is widely used as a reporter protein because it has high sensitivity and a broad linear range. In the commonly used reporter assay, β-galactosidase, a well-characterized bacterial enzyme, or renilla luciferase is usually used in conjunction with firefly luciferase to normalize the transfection efficiency of the reporter gene (Sherf et al., 1996; Martin et al., 1996). In such cases, the activity of the two reporter proteins must be measured in different ways (e.g., absorptiometry and luminescence photometry) or by using two substrates. In the reporter assay presented here, we used two species derived from green fluorescent protein (GFP), one (enhanced yellow fluorescent protein, (EYFP)) to measure the promotion and enhancement of gene expression, and the other (enhanced cyan fluorescent protein, (ECFP)) to normalize the transfection, and were thus able to measure the fluorescent protein signals simultaneously without any co-factor or substrates. As a result of screening of more than 140 compounds, it was found that several compounds activate RARs and/or FXR.

Materials and methods

Chemicals

Chenodeoxycholic acid was purchased from Sigma-Aldrich (St. Louis, MI, USA), and ATRA and 9CRA were from Wako (Osaka, Japan). Ginkgolic acid 17:1, 15:0, and 13:0 were purchased from Nagara Science (Gifu, Japan).

Purification and synthesis of test compounds

Ginkgolic acid 15:1 was purified from *Ginkgo biloba L.* var. *diptera* according to Morimoto et al. (1968). 2-Methyl ginkgolic acid methyl ester was prepared by methylation of the ginkgolic acid with methyl iodide and K_2CO_3 (Paul and Yeddanapalli, 1956; Begum et al., 2002). Grifolin was purified from *Albatrellus confluens* and *Albatrellus ovinus* (Ishii et al., 1988; Nukata et al., 2002). We isolated bazzanenyl caffeate from the liverwort *Bazzania fauriana* (Toyota and Asakawa, 1988). We synthesized caffeic acid phenethyl ester (CAPE), farnesyl caffeate and geranyl caffeate for acquirement in quantity. The synthesis of CAPE by coupling reactions of caffeic acid and β-phenylethyl bromide was reported by Hashimoto et al. (1988), and the details of the synthesis of farnesyl and geranyl caffeates are described below. The purity of the compounds for the bioactivation test was shown to be over 95% by ^1H and ^{13}C NMR spectra.

Synthesis of farnesyl caffeate

Twenty-five percent NaOH (2.5 ml) was added to a solution of caffeic acid (3,4-dihydroxycinnamic acid) (2.10 g) in HMPA (hexamethylphosphoric triamide) (150 ml), and the mixture was stirred for 1 h under N_2 at room temperature. A solution of farnesyl bromide (4.98 g) in HMPA (20 ml) was added dropwise for

10 min to the reaction mixture. The reaction mixture was stirred for 24 h at room temperature, and poured in ice cold H_2O (300 ml). The organic layer, which was extracted with Et_2O (200 ml × 2), was washed with brine (300 ml), dried ($MgSO_4$) and evaporated under reduced pressure to an oil (6.75 g). The oil was chromatographed on silica gel (200 g) with a gradient solvent system of $CHCl_3$–EtOAc, increasing the amount of 2% portions EtOAc stepwise to give 32 fractions. Farnesyl caffeate (1.435 g; Y. 43.2%) was obtained from 10% EtOAc-*n*-hexane eluate (Fr. 12-18) as a pure white powder. Caffeic acid (1.025 g; Y. 48.8%), the starting material, was recovered from 20% EtOAc-*n*-hexane eluate (Fr. 25-31).

Farnesyl caffeate: EI-MS: *m/z* 384 (M^+,5%), 315, 204, 180, 163 (100%), 135, 93, 69; HR-MS: *m/z* 384.2307, $C_{24}H_{32}O_4$ requires 384.2300; anal. calcd. for $C_{24}H_{32}O_4$: C, 74.97; H, 8.39. Found: C, 74.85; H, 8.30; FT-IR (KBr) cm^{-1}: 3480 (OH), 3301 (OH), 1678 (C=O), 1600, 1278, 1183; UV (EtOH) λ_{max} nm (log ε): 333 (4.15), 303 (4.00), 248 (3.90), 220 (4.03); ^{1}H NMR (acetone-d_6): δ1.56 (3H, *s*, CH_3), 1.62 (3H, *s*, CH_3), 1.65 (3H, *s*, CH_3), 1.76 (3H, *s*, CH_3), 4.68 (1H, *d*, *J* = 7.0 Hz, H-1′), 5.12 (2H, *m*, H-6′ and H-10′), 5.41 (1H, *t*, *J* = 7.0 Hz, H-2′), 6.26 (1H, *d*, *J* = 15.9 Hz, H-β), 6.87 (1H, *d*, *J* = 8.2 Hz, H-5), 7.03 (1H, *dd*, *J* = 1.8, 8.2 Hz, H-6), 7.15 (1H, *d*, *J* = 1.8 Hz, H-2), 7.53 (1H, *d*, *J* = 15.9 Hz, H-α), 8.26 (1H, *br.s*, –OH), 8.49 (1H, *br.s*, –OH); ^{13}C NMR ((acetone-d_6): δ16.1 (*q*, CH_3), 16.4 (*q*, CH_3), 17.7 (*q*, CH_3), 25.8 (*q*, CH_3), 26.8 (*t*, CH_2), 27.4 (*t*, CH_2), 40.1 (*t*, CH_2), 40.4 (*t*, CH_2), 61.3 (*t*, CH_2), 115.1 (*d*, CH), 115.7 (*d*, CH), 116.3 (*d*, CH), 120.1 (*d*, CH), 122.4 (*d*, CH), 124.6 (*d*, CH), 125.1 (*d*, CH), 127.6 (*s*, C), 131.6 (*s*, C), 135.9 (*s*, C), 142.1 (*s*, C), 145.6 (*d*, CH), 146.3 (*s*, C), 148.7 (*s*, C), 167.3 (*s*, –COO)).

Synthesis of geranyl caffeate

Twenty-five percent NaOH (2.1 ml) was added to a solution of caffeic acid (2.00 g) in HMPA (150 ml), and the mixture was stirred for 1 h under N_2 at room temperature. A solution of geranyl bromide (3.10 g) in HMPA (20 ml) was added dropwise for 10 min to the reaction mixture. The reaction mixture was treated further as described above to afford geranyl caffeate (1.48 g; Y. 61.4%) as a white powder, and caffeic acid (0.56 g; Y. 28.0%).

Geranyl caffeate: EI-MS: *m/z* 316 (M^+, 10%), 247, 180, 163 (100%), 136, 69; HR-MS: *m/z* 316.1682, $C_{19}H_{24}O_4$ requires 316.1674; anal. calcd. for $C_{19}H_{24}O_4$: C, 72.12; H, 7.65. Found: C, 72.01; H, 7.68; FT-IR (KBr) cm^{-1}: 3483 (OH), 3295 (OH), 1678 (C=O), 1599, 1278, 1183; UV (EtOH) λ_{max} nm (log ε): 334 (4.16), 302 (4.05), 249 (3.93), 222 (4.01); ^{1}H NMR (acetone-d_6): δ1.60 (3H, *s*, CH_3), 1.66 (3H, *s*, CH_3), 1.75 (3H, *s*, CH_3), 4.68 (1H, *d*, *J* = 7.0 Hz, H-1′), 5.12 (1H, *t*, *J* = 7.0 Hz, H-6′), 5.40 (1H, *t*, *J* = 7.0 Hz, H-2′), 6.27 (1H, *d*, *J* = 15.9 Hz, H-β), 6.87 (1H, *d*, *J* = 8.2 Hz, H-5), 7.03 (1H, *dd*, *J* = 2.0, 8.2 Hz, H-6), 7.16 (1H, *d*, *J* = 2.0 Hz, H-2), 7.55 (1H, *d*, *J* = 15.9 Hz, H-α), 8.28 (1H, *br.s*, –OH), 8.50 (1H, *br.s*, –OH); ^{13}C NMR ((acetone-d_6): δ16.4 (*q*, CH_3), 17.7(*q*, CH_3), 25.8 (*q*, CH_3), 27.0 (*t*, CH_2), 40.1 (*t*, CH_2), 61.3 (*t*, CH_2), 115.1 (*d*, CH), 115.6 (*d*, CH), 116.3 (*d*, CH), 120.0 (*d*, CH), 122.4 (*d*, CH), 124.6 (*d*, CH), 127.6 (*s*, C), 132.0 (*s*, C), 142.1 (*s*, C), 145.6 (*d*, CH), 146.3 (*s*, C), 148.7 (*s*, C), 167.3 (*s*, –COO)).

Plasmid construction

Plasmids were constructed for the expression of RXRα, FXR and RARs. The ORF regions of human RXRα, human FXR, mouse RARα1, mouse RARβ2, and mouse RARγ1 (accession numbers X52773, U68233, X57528, S56660, X15848) were amplified by PCR and inserted into pcDNA3.1 (Invitrogen, Carlsbad, CA, USA), respectively. For reporter plasmids, the luciferase region of the pGL3-Control Vector (Promega, Madison, WI, USA) was replaced with the EYFP fragment of pEYFP-N1 or the ECFP fragment of pECFP-N1 (Clontech, Palo Alto, CA, USA) using *Nco*I and *Xba*I sites. Subsequently, the simian virus 40 (SV40) early promoter was cut out with *Bgl*II and *Hin*dIII, and replaced with the thymidine kinase (TK) promoter of the pRL-TK vector (Promega) or one of several other promoters (the 3′ region of the TK promoter, the cytomegalovirus (CMV) promoter, or the minimal CMV promoter and the 3′ region of the CMV promoter (201 and 265 bp)) amplified using the following PCR primers:

5′-ggagatctggccccgcccagcgtcttgtc-3′ and 5′-ggaagcttgcggcacgctgttgacgctgttaagcgggtcgctgcaggg-3′ (3′ region of the TK promoter);
5′-ccagatcttagttattaatagtaatcaattacggggtc-3′ and 5′-ccaagcttgatctgacggttcactaaaccagc-3′ (CMV promoter);
5′-ccagatcttaggcgtgtacggtgggagg-3′ and 5′-ccaagcttaggctggatcggtcccggtg-3′ (minimal CMV promoter);
5′-ccagatcttgggagtttgttttggcacc-3′ and reverse primer of CMV promoter (CMV 201); and
5′-ccagatcttcaatgggcgtggatagcgg-3′ and reverse primer of CMV promoter (CMV265).

Double-stranded oligonucleotides containing HREs (RXRE, RARE and FXRE; shown in Fig. 1B) were ligated into the upstream region of these promoters using *Mlu*I and *Bgl*II sites. The sequences of the constructed plasmids were confirmed by sequencing using an ABI PRISM 310 Genetic Analyzer (Applied Biosystems, Foster City, CA, USA).